

Photo-Activatable Substrates for Site-Specific Differentiation of Stem Cells

Kai Han,^{†,‡} Wei-Na Yin,[†] Jin-Xuan Fan,[†] Feng-Yi Cao,[†] and Xian-Zheng Zhang^{*,†}

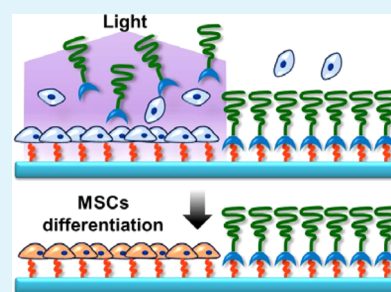
[†]Key Laboratory of Biomedical Polymers of Ministry of Education and Department of Chemistry, Wuhan University, Wuhan 430072, China

[‡]College of Science, Huazhong Agricultural University, Wuhan 430070, China

Supporting Information

ABSTRACT: In this report, a UV sensitive, PEGylated PFSSTKTC (Pro-Phe-Ser-Ser-Thr-Lys-Thr-Cys) peptide was modified on quartz substrate to investigate the spatial controlled differentiation of stem cells. This substrate could restrict the cell adhesion due to the steric hindrance of PEG shell. With UV irradiation, PFSSTKTC became exposed owing to the breakage of o-nitrobenzyl group with the detachment of PEG shell. The irradiation boundary on substrate was stable in the long term. The *in vitro* osteogenic differentiation results revealed that under the site-specific irradiation, the mesenchymal stem cells (MSCs) could specifically differentiate into osteoblast under the induction of PFSSTKTC peptide. This photoactivatable biomaterial shows great potential for region controllable and precise MSCs differentiation.

KEYWORDS: stem cells, osteogenic differentiation, photoactivatable, cell adhesion, site-specific



1. INTRODUCTION

Stem cells have presented great potential in tissues or organs restoration and regeneration medicine since they can self-renew continuously and differentiate into several lineages such as adipocytes and osteoblasts.^{1–4} Regulating the differential behaviors of stem cells precisely has attracted extensive research interest. To date, various regulatory factors, such as physical factors, soluble factors, cell–cell interactions, and cell–biomaterial interactions, have been investigated via fabrication of various bionic biomaterials.^{5–8} For example, Ding et al. developed a series of elegant micropatterned material surfaces to reveal the effects of aspect ratio of cells and cell–cell contact on the differentiation of stem cells.⁹ Great success has been achieved; however, the creation of these biomaterials is still complicated and tedious. On the other hand, the existing works are mainly focused on exploration of potential factors on adherent stem cells, where biomaterials are always static during the incubation. Very little work has been done about the influence of spatially dynamic controlled adhesion on biomaterials to the differentiation of stem cells. It was recognized that cell adhesion has profound effects on the cell fate and cellular responses.¹⁰ In addition, spatially controlled stem cell adhesion is also critically important to achieve site-specific differentiation of stem cells on-demand.

To realize the spatially dynamic control of cell adhesion, many strategies have been proposed, and the cell adhesion behaviors can be regulated by external stimuli such as enzyme, heat, and voltage.^{11–13} Among these external stimuli, light as a high spatiotemporal resolved energy source is noninvasive and has attracted extensive attention.¹⁴ Meanwhile, photoinduced structural transformation or photochemical reaction can be finished in a very short time via regulating the light irradiation

conditions such as intensity and wavelength.¹⁵ For example, Nakanishi et al. developed a substrate coated with protein that could prevent cell adhesion. With light irradiation, the protein shell was replaced with promoting cell adhesion.¹⁶ In our previous report, we fabricated a photoresponsive “smart template” for reversible cell adhesion based on host–guest interaction.¹⁷ However, these light mediated spatial controlled substrates have been scarcely used, thus far, for manipulating the differentiation of stem cells.

In this work, we fabricate a simple but effective self-assembly monolayer (SAM) for the photoactivatable, site-specific differentiation of stem cells. As shown in Figure 1, quartz substrate was modified with PFSSTKTC (Pro-Phe-Ser-Ser-Thr-Lys-Thr-Cys) peptide and PEG₅₀₀₀ using o-nitrobenzyl group as a UV-sensitive linker. The PEG shell would block the adhesion of stem cells on substrate. Upon regional UV irradiation, the photolytic reaction will lead to the detachment of PEG shell, and expose PFSSTKTC peptide, which has been confirmed to be able to mediate the differentiation of stem cells.^{18,19} It was envisioned that stem cells could anchor on the substrate and differentiate into certain cell-lines under the induction of PFSSTKTC peptide. The site-specific differentiation of stem cells was investigated in terms of Alizarin Red S staining, immunofluorescence of osteopontin (OPN), and so on.

Received: August 12, 2015

Accepted: October 9, 2015

Published: October 9, 2015

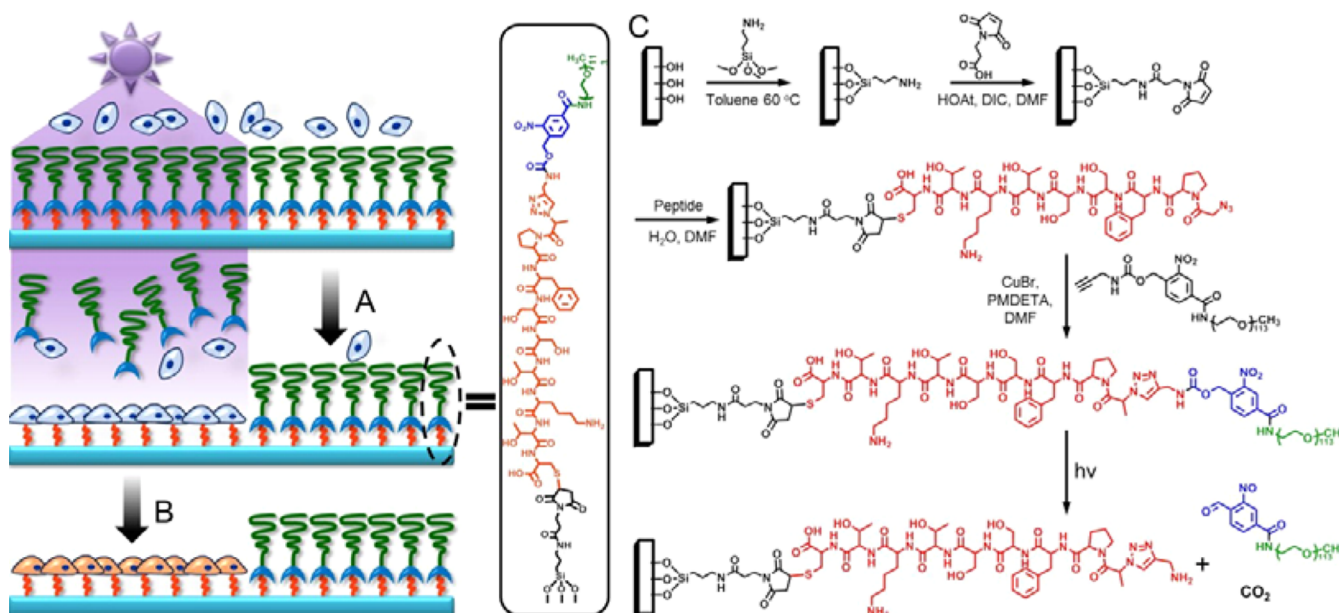


Figure 1. Schematic illustration of photoactivatable MSCs release and osteogenic differentiation on functionalized substrates: (A) UV light triggered detachment of PEG shell and the enhanced cell adhesion to substrate in this region; (B) osteogenic differentiation of MSCs mediated by PFSSTKTC peptide. (C) Layer-by-layer modification of quartz substrates and working principle of phototriggered release of PEG segment.

2. EXPERIMENTAL SECTION

2.1. Materials. Detailed information on materials was supported in our previous article.²⁰ Additionally, 4-(bromomethyl)-3-nitrobenzoic acid, 3-aminopropyltrimethoxysilane, and 3-maleimidopropionic acid were provided by J&K Chemical (China). Triphosgene, 2-propynylamine, *N,N'*-diisopropylcarbodiimide (DIC), and *N,N,N',N''*-pentamethyldiethylenetriamine (PMDETA) were purchased from Aladdin Industrial Corporation (China). mPEG-NH₂ (M_w = 5000) was obtained from YARE biotechnology Corporation (Shanghai, China) and used without further purification. Triton X-100 was provided by Biosharp. CF488A-Phalloidin was provided by Biotium. Goat antirabbit IgG-Cy3 was provided by Boster.

2.2. Synthesis of Compound 2 (4-(Hydroxymethyl)-3-nitrobenzoic acid). The synthetic process of compound 2 was based on previous report.²¹ The 4-(bromomethyl)-3-nitrobenzoic acid (1) (1.01 g, 3.88 mmol) and Na₂CO₃ (2.68 g, 13.6 mmol) were dissolved in 30 mL of acetone/H₂O (1:1). The solution was refluxed overnight. Subsequently, acetone was removed. The residual solution was extracted with 5 mL of diethyl ether twice. Then HCl solution was added, and a lot of yellow precipitate appeared. The aqueous phase was extracted with ethyl acetate (20 mL) two times. The solid was redissolved in ethyl acetate (20 mL). The combined organic phase was washed with DI water, and then MgSO₄ was added. The solution was evaporated, and compound 2 was obtained as a yellow solid.

2.3. Synthesis of Compound 3. mPEG₅₀₀₀-NH₂ and compound 2 were dissolved in 15 mL of DMF. Then PyBOP and diisopropylethylamine (DIEA) were added to the solution. After the reaction for 48 h under nitrogen atmosphere, the solution was dialyzed for 3 days (MWCO 1000). The solution was freeze-dried to get compound 3.

2.4. Synthesis of Compound 4. Under nitrogen atmosphere, compound 3 and phosgene were dissolved in 20 mL of CH₂Cl₂. Then DIEA was added. The solution was vigorously stirred for 3 h. Unreacted phosgene gas was removed via flushing with nitrogen gas. Subsequently, propargylamine in CH₂Cl₂ was added to the above solution. The reaction mixture was further stirred for 24 h. The solvent was evaporated off and dialyzed for 3 days (MWCO 1000). The solution was subsequently freeze-dried to obtain compound 4.

2.5. Synthesis of Peptide. The peptide N₃-PFSSTKTC was synthesized based on solid phase synthesis method.²⁰ *N*-Fluorenyl-9-methoxycarbonyl (Fmoc) protected amino acids were conjugated to 2-chlorotriethyl chloride resin using HOBt/HBTU/DIEA as coupling

reagents. A 20% piperidine/DMF (v/v) solution was employed to cleave the Fmoc group and expose the amino group. The peptide was cleaved from 2-chlorotriethyl chloride resin in a mixture of trifluoroacetic acid, H₂O, and triisopropylsilane for 1.5 h. The volume ratio was 95:2.5:2.5. The solution was concentrated. The solution was added to diethyl ether, and white solid formed. The product was dried under vacuum.

2.6. Surface Preparation. The 3-maleimidopropionic acid modified quartz substrates were prepared as our previous work.¹⁹ Peptide was anchored to the substrates via Michael addition reaction, that is, incubating peptide solution with quartz substrates at room temperature for 48 h. Then substrates were repeatedly washed with methylbenzene, DI water, and ethanol, respectively. Quartz substrates were dried under vacuum. To introduce the UV-sensitive PEG, the quartz substrates were immersed in DMF. Then compound 4, CuBr, and PMDETA were added and stirred under the argon atmosphere for 72 h. Before the further characterizations, quartz substrates were repeatedly washed and then dried under vacuum. The substrates were characterized in terms of XPS (X-ray photoelectron spectroscopy) and CA (contact angle) measurements. The detailed preparation process of the SAM-substrates is shown in Figure 1.

2.7. Cell Culture. We extracted MSCs from the bone marrow of mature rats (Sprague–Dawley). MSCs (passage 2) were seeded on the substrates, and the density of MSCs was 20 000 cells per milliliter. MSCs and COS7 cells were both incubated in DMEM with 10% fetal bovine serum and 1% penicillin–streptomycin (inhibit the growth of germ) at 37 °C in a 5% CO₂ atmosphere.

2.8. Cells Adhesion. COS7 cells were seeded on PU-SAM modified substrates. Twenty-four hours later, half of the PU-SAM substrates were illuminated with UV light for total 5 min (30 s of irradiation, and then 30 s of interval (nonirradiation) between irradiations, $\lambda = 365$ nm, intensity was 72 mJ/cm²) by photomasks. Subsequently, the cells were further incubated for preset times and imaged via fluorescence inversion microscope system. Before that, cells were gently washed with PBS buffer repeatedly.

2.9. Stem Cell Proliferation. MSCs were seeded on PU-SAM modified substrates. After 24 h of incubation, the PU-SAM substrates received UV light for 0 or 5 min. Twenty-four hours later, MSCs cells were gently washed with DMEM and then cultured for another 3 or 6 days. Subsequently, 5 mg/mL of MTT was added to the culture medium. After 4 h of incubation, the medium was extracted, and

dimethyl sulfoxide (DMSO) was added to each well. The solution was positioned into 96-well plates. A microplate reader was employed to detect the absorbance at 570 nm. The relative cell viability was measured via choosing the OD value (representation of cell number) of cells on the quartz substrate without UV light irradiation at the third day as 100%.

2.10. Alizarin Red S Staining. MSCs were incubated on PU-SAM modified substrates. After 24 h of incubation, half of PU-SAM substrates were exposed to UV light for 5 min by photomasks. Twenty-four hours later, cells were washed many times with PBS buffer to remove the detached PEG segment and further incubated for 6 days. Thereafter, the substrates were repeatedly washed with PBS, and MSCs were immersed in para-formaldehyde solution to fix MSCs. Then Alizarin Red S in Tris-HCl buffer (w/v 1%) was added to the substrates for 30 min. The substrates were washed with PBS buffer before the further measurement via fluorescence inversion microscope system.

2.11. Immunofluorescence of Osteopontin. The MSCs incubation and fixation procedures were conducted according to the Alizarin Red S staining experiment. Then the substrates were rinsed with PBS for three times. The substrates were cultured in PBS solution containing Triton-X 100. Ten minutes later, the substrates were repeatedly washed with PBS and then immersed in PBS solution containing 3% BSA to block nonspecific sites at room temperature for 1 h. CF488A-Phalloidin was used to label the F-actin. Cells were washed four times with PBS and then cultured with an osteopontin (OPN) antibody (1:100 dilution). One hour later, the substrates were repeatedly washed with PBS, and then antirabbit IgG-Cy3 (1/100 dilution) was added to the substrates. Thirty minutes later, the substrates were repeatedly washed. Immunofluorescence stain of MSCs was directly observed via CLSM (confocal laser scanning microscopy). Furthermore, the osteopontin fluorescence signal was semiquantified via ImageJ software.

3. RESULTS AND DISCUSSION

3.1. Characterization of PEGylated UV-Responsive, SAM-Modified Substrate. PEGylated UV responsive SAM (PU-SAM) on quartz substrate was obtained by a layer-by-layer strategy. The detailed fabrication of PU-SAM was presented in Figure 1. Briefly, peptide linker N_3 -PFSSTKTC was prepared via a standard solid phase peptide synthesis method (ESI-MS in Figure S1, see Supporting Information), and then peptide self-assembly monolayer (P-SAM) formed on maleinimide modified substrate via Michael addition reaction. Thereafter, alkylnated UV photocleavage PEG₅₀₀₀ was synthesized (Figure S2). PU-SAM was obtained via the Click reaction between P-SAM and alkylnated PEG₅₀₀₀. The detailed alkylnation process of PEG was monitored by ¹H NMR and FT-IR spectra (Figure S3). The FT-IR peak of alkyne group at 2113 cm⁻¹ indicated the successful alkylnation of UV photocleavage PEG₅₀₀₀.

Considering that the layer-by-layer modified substrates possessed different hydrophilic properties, contact angle (CA) was measured to verify the surface modification of different substrates. Water drops images on various surfaces were shown in Figure 2. Because of the abundant hydrophilic hydroxyl groups, the CA of "piranha" solution treated quartz surface was just $6.5 \pm 1.7^\circ$ (Figure 2A). After reacting with 3-aminopropyltrimethoxysilane, the CA increased to $33.9 \pm 3.2^\circ$ (Figure 2B). The following modification of maleinimide groups further increased the CA up to $41.8 \pm 2.4^\circ$ (Figure 2C) since maleinimide groups had stronger hydrophobicity than amino groups. Then, N_3 -PFSSTKTC peptide was anchored via Click reaction (P-SAM), which decreased the CA to $30.8 \pm 2.2^\circ$ (Figure 2D). Meanwhile, formation of PU-SAM further reduced the surface hydrophobicity of substrate dramatically,

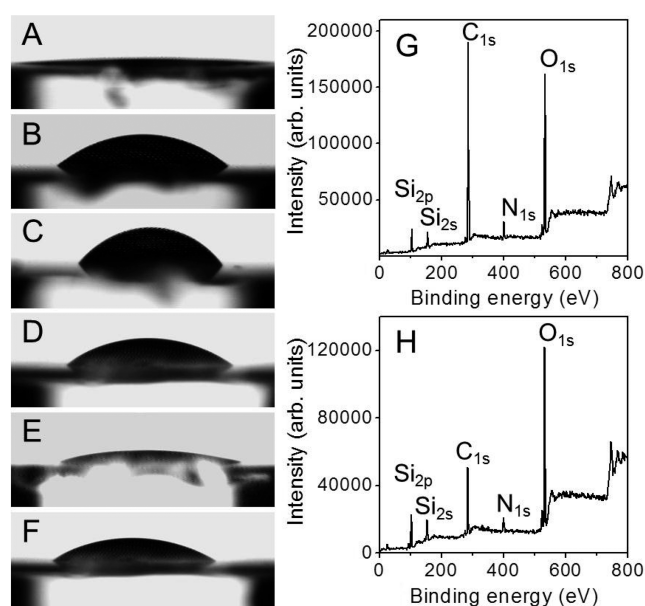


Figure 2. CA measurement of various substrates: (A) "piranha" solution treated substrate, (B) amino-modified substrate, (C) maleinimide-modified substrate, (D) P-SAM modified substrate, (E) PU-SAM modified substrate, and (F) PU-SAM modified substrate with UV light irradiation. XPS analysis of PU-SAM modified substrate (G) before and (H) after UV light irradiation.

whose CA value was $11.6 \pm 1.3^\circ$ (Figure 2E), which disfavored the cell adhesion. These changing in CA values substantially demonstrated the successful fabrication of PU-SAM. Additionally, the CA restored to $28.7 \pm 1.7^\circ$, which was very close to that observed in P-SAM modified substrate when the PU-SAM modified substrate received UV irradiation (Figure 2F). Undoubtedly, photolytic reaction of photosensitive linker (o-nitrobenzyl group) detached PEG shell and exposed peptide, which would enhance the hydrophobicity of substrates. It was known that hydrophobic surface would benefit cell adhesion.^{22,23}

Furthermore, XPS spectral was conducted to analyze the change of C, N, O, and Si elements on the surface of different substrates. It was found that the peaks of O_{1s}, Si_{2s}, and Si_{2p} were very strong on surface of blank substrate due to the existing of silanol groups (Figure S4A). The programmed modification of maleinimide group (Figure S4B) and PFSSTKTC peptide (Figure S4C) on the substrates increased the relative intensity of C_{1s} and N_{1s}. Once the PEG segment was introduced, the relative intensity of C_{1s} and O_{1s} increased dramatically. Clearly, modification of PEG segment significantly enhanced the content of C and O elements on the substrate surface (Figure 2G). When the PU-SAM modified substrates were treated by UV light irradiation, as expected, the intensity of C_{1s} and O_{1s} decreased significantly (Figure 2H). The tendency of XPS was similar to that of CA measurement. Both the CA and XPS results demonstrated the successful formation of photoactivatable PU-SAM on the substrate.

3.2. Photo-Activatable Adhesion of Stem Cells. Encouraged by the photoactivatable PEG detachment on substrate, the photo manipulated cell adhesion behaviors were investigated using COS7 (African green monkey SV40-transfected kidney fibroblast cell line) as the cell model. Here, COS7 cells but not stem cells were chosen for the experiment cells due to their faster adhesion and proliferation, which was

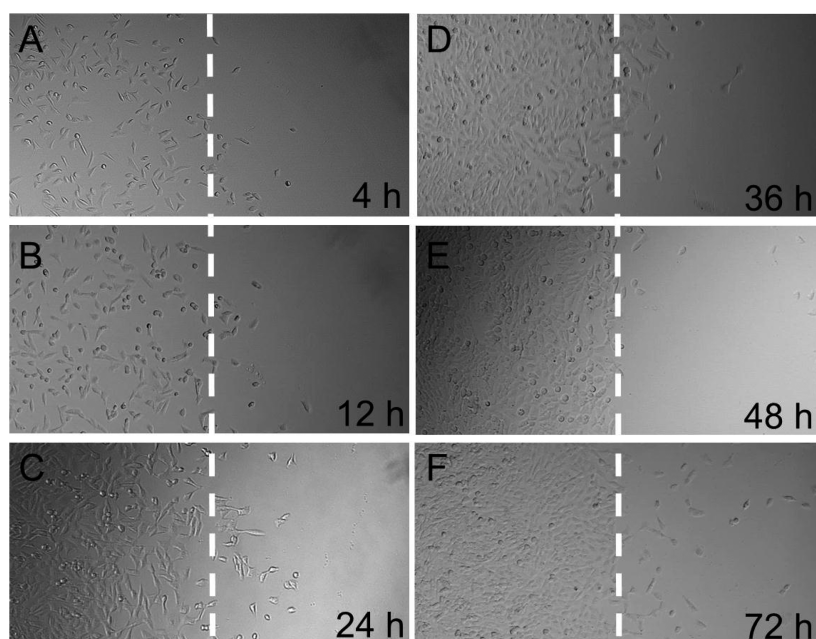


Figure 3. Images of cell release on PU-SAM modified substrate in the presence of light irradiation (left side) or absence of light irradiation (right side) at various times: (A) 4 h, (B) 12 h, (C) 24 h, (D) 36 h, (E) 48 h, and (F) 72 h.

more appropriate for photolytic induced adhesion investigation in a short period. Meanwhile, the result of cell viability confirmed that UV light irradiation with appropriate time would not significantly inhibit the growth of stem cells (Figure S5). Considering that PEG shell would gradually fall out with the increase of irradiation time, which weakened the cell adhesion on substrate, herein, the principle of choosing irradiation time was to decrease the harm of UV light irradiation to cells furthest while realizing the detachment of PEG shell. As shown in Figure 3, a few cells were observed in the nonirradiation region. In sharp contrast, COS7 cells selectively attached to the irradiated region on PU-SAM modified substrate and well-defined cell patterns were obtained from 4 h. Meanwhile, the cell number increased with time prolonging. Similar cell adhesion behavior was also observed on cells that were cultured on peptide-only modified substrate (negative control, Figure S6). Furthermore, quantitative analysis of cell number on PU-SAM modified substrates with or without UV irradiation was also performed in Figure S7. Note that COS7 cells were still confined in the photoactivated patterns, and the boundary of the pattern remained clear even at 72 h. These results were due to the fact that although PEG did not affect biochemical functionality of cells, the lack of ionic interaction between PEG film and the nearby cells and steric repulsion exerted by PEG film dramatically decreased protein adsorption as well as cell attachment on PU-SAM modified substrate.^{24,25} When PU-SAM modified substrate received UV irradiation, photolytic reaction occurred. More hydrophobic PFSSTKTC peptide emerged, which was in favor of cell adhesion.

To evaluate the photo-manipulated adhesion for long-term effect, cell proliferation behaviors were measured via MTT assay. MSCs were chosen as stem cell model because MSCs could be isolated from various tissues with ease such as bone marrow, brain, heart, and muscle. Meanwhile, MSCs can be readily expanded *in vitro*. It was found that the cell proliferation on PU-SAM modified substrate with UV irradiation was

significantly higher than that without UV irradiation since MSCs could not adhere and proliferate on PU-SAM modified substrate efficiently due to the existence of PEG shell. Obviously, the tendency of proliferation of MSCs was similar to that of COS7 adhesion. Additionally, it was found that prolonging the incubation time from 3 days to 6 days increased the amount of stem cells on the substrate with UV irradiation (Figure 4), while no change was found in the group without light irradiation.

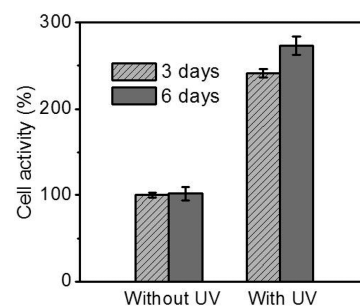


Figure 4. MSCs proliferation behaviors on PU-SAM modified substrates with or without light irradiation at different times.

3.3. Osteogenic Differentiation of MSCs on PU-SAM Modified Substrate. On PU-SAM modified substrate, PFSSTKT peptide was introduced to aim at mediating the MSCs differentiation. As a peptide sequence derived from the bone marrow homing peptide 1, PFSSTKT peptide is abundant in S, K, T, P, and F amino acids, which is able to target bone marrow as well as bind to stem cells.¹⁸ Also, our previous study has proved that PFSSTKT peptide could promote osteogenic differentiation of stem cells.¹⁹ To verify whether PU-SAM modified substrate can achieve site-specific MSCs differentiation, Alizarin Red S staining was conducted to evaluate the MSCs mineralization. Since Ca^{2+} could affect the proliferation and osteogenic differentiation behavior, gene and protein expression of MSCs, calcium deposition or cell

mineralization was recognized as a crucial indicator for mature osteoblasts.²⁶ Alizarin Red S staining was used for the indicator of mineralization owing to its selectively binding to the calcium salts, which directly visualized extracellular calcium deposition. After 6-day incubation, according to the result of Alizarin Red S staining (Figure 5), nearly no red signal was found at the right

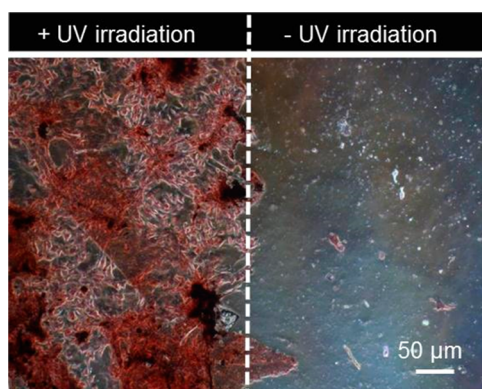


Figure 5. Microscopy image of the calcium deposition at the sixth day via Alizarin Red S staining. MSCs were incubated on PU-SAM modified substrates with or without light irradiation.

side of the boundary, where no UV light irradiation was performed. On the contrary, in the left region with UV light irradiation, obvious red signal was found, which was similar to the result that was observed on PFSSTKTC peptide modified substrates (Figure S8). Meanwhile, significant calcium nodules were found, which confirmed that the PEG shell detachment and subsequent exposure of PFSSTKTC peptide were in favor of cell adhesion. Then PFSSTKTC peptide further induced osteogenic differentiation as well as promoted bone formation site-specifically.

To further confirm the site-specific osteogenic differentiation, OPN expression was observed via CLSM. OPN as an important late osteogenic biomarker was upregulated during osteogenic differentiation.^{27,28} Herein, OPN was labeled with red fluorescence (Cy3), while F-actin was stained with green fluorescence. Before light irradiation, OPN expression of MSCs on PFSSTKTC peptide modified substrates at the third and sixth day was observed. Figure S9 revealed that PFSSTKTC peptide could successfully mediate the expression of OPN. Thereafter, UV light irradiation was performed. As shown in Figure 6, due to the poor cell adhesion, the right region without UV light irradiation had no red signal; even the peptide that could mediate the differentiation of MSCs existed. However, strong red signal was found in the left region with UV light irradiation, indicating the emergence of OPN. It was clear that the detachment of PEG exposed PFSSTKTC peptide. More importantly, the detachment of PEG increased the hydrophobicity of substrate, leading to enhanced cell–substrate contact, which was indispensable in differentiation of MSCs. Meanwhile, the expression of OPN increased when the cultivation time of MSCs was prolonged from 3 days to 6 days, while the boundary was still clear. Furthermore, the OPN expression of MSCs was semiquantified. The mean fluorescence intensity of red signal (OPN expression) with UV light irradiation was significantly higher than that without light irradiation for 3 days and 6 days (Figure 6A4,B4). Taken together, PU-SAM modified substrate that possessed UV light

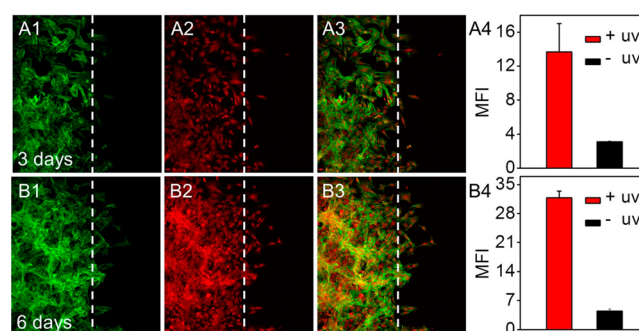


Figure 6. OPN expression of MSCs at the (A1–A3) third day and (B1–B3) sixth day via immunofluorescent staining was observed by CLSM. The left side of the white line was with light irradiation, while the right side was without light irradiation. Green signal, filamentous actin; red signal, osteopontin. A4 and B4: mean fluorescence intensity of A2 and A3, which was determined via ImageJ software.

controlled cell adhesion property realized site-specific differentiation of MSCs.

4. CONCLUSION

In summary, a photoactivatable substrate was fabricated and realized site-specific differentiation of MSCs. This substrate underwent the illumination-triggered PEG detachment. The enhanced hydrophobicity was in favor of MSCs adhesion to substrate, which promoted peptide mediated differentiation of MSCs. In addition, this site-specific differentiation effect of stem cells in the presence of light irradiation was stable for a relatively long time. The photoactivatable strategy demonstrated here opens a window in spatial controlled differentiation of stem cells and should have great potential in region-controllable regeneration medicine.

■ ASSOCIATED CONTENT

Supporting Information

The Supporting Information is available free of charge on the ACS Publications website at DOI: 10.1021/acsami.5b07455.

Scheme of fabrication of PU-SAM modified substrate; UV-activatable alkynylated PEG; ESI-MS of peptide; ¹H NMR spectra of compounds 2 and 3; FT-IR spectra of compounds 3 and 4; XPS analysis of blank quartz substrate, maleinimide-terminated substrate, and P-SAM modified substrate; cell viability of stem cells under UV light irradiation; cell adhesion of COS7 cells on PFSSTKTC peptide modified substrate; quantitative analysis of cell number on PU-SAM modified substrates with or without UV irradiation; calcium deposition and osteopontin expression of stem cells on PFSSTKTC peptide modified substrate (PDF)

■ AUTHOR INFORMATION

Corresponding Author

*E-mail: xz-zhang@whu.edu.cn.

Notes

The authors declare no competing financial interest.

■ ACKNOWLEDGMENTS

This work was supported by the National Natural Science Foundation of China (51125014, 51233003, and 21474077)

and the Ministry of Science and Technology of China (2011CB606202).

REFERENCES

- (1) Jiang, Y. H.; Jahagirdar, B. N.; Reinhardt, R. L.; Schwartz, R. E.; Keene, C. D.; Ortiz-Gonzalez, X. R.; Reyes, M.; Lenvik, T.; Lund, T.; Blackstad, M.; Du, J. B.; Aldrich, S.; Lisberg, A.; Low, W. C.; Largaespada, D. A.; Verfaillie, C. M. Pluripotency of Mesenchymal Stem Cells Derived from Adult Marrow. *Nature* **2002**, *418*, 41–49.
- (2) Engler, A. J.; Sen, S.; Sweeney, H. L.; Discher, D. E. Matrix Elasticity Directs Stem Cell Lineage Specification. *Cell* **2006**, *126*, 677–689.
- (3) Oswald, J.; Boxberger, S.; Jørgensen, B.; Feldmann, S.; Ehninger, G.; Bornhäuser, M.; Werner, C. Mesenchymal Stem Cells Can Be Differentiated into Endothelial Cells *in Vitro*. *Stem Cells* **2004**, *22*, 377–384.
- (4) Crisan, M.; Yap, S.; Casteilla, L.; Chen, C. W.; Corselli, M.; Park, T. S.; Andriolo, G.; Sun, B.; Zheng, B.; Zhang, Li.; Norotte, C.; Teng, P. N.; Traas, J.; Schugar, R.; Deasy, B. M.; Badyrak, S.; Bühring, H.-J.; Jacobino, J.-P.; Lazzari, L.; Huard, J.; Peault, B. A Perivascular Origin for Mesenchymal Stem Cells in Multiple Human Organs. *Cell Stem Cell* **2008**, *3*, 301–313.
- (5) Higuchi, A.; Ling, Q. D.; Hsu, S. T.; Umezawa, A. Biomimetic Cell Culture Proteins as Extracellular Matrices for Stem Cell Differentiation. *Chem. Rev.* **2012**, *112*, 4507–4540.
- (6) Ying, Q. L.; Nichols, J.; Chambers, I.; Smith, A. BMP Induction of Id Proteins Suppresses Differentiation and Sustains Embryonic Stem Cell Self-Renewal in Collaboration with STAT3. *Cell* **2003**, *115*, 281–292.
- (7) Liao, S. S.; Nguyen, L. T. H.; Ngiam, M.; Wang, C.; Cheng, Z. Y.; Chan, C. K.; Ramakrishna, S. Biomimetic Nanocomposites to Control Osteogenic Differentiation of Human Mesenchymal Stem Cells. *Adv. Healthcare Mater.* **2014**, *3*, 737–751.
- (8) Tang, J.; Peng, R.; Ding, J. D. The Regulation of Stem Cell Differentiation by Cell-Cell Contact on Micropatterned Material Surfaces. *Biomaterials* **2010**, *31*, 2470–2476.
- (9) Peng, R.; Yao, X.; Ding, J. D. Effect of Cell Anisotropy on Differentiation of Stem Cells on Micropatterned Surfaces through the Controlled Single Cell Adhesion. *Biomaterials* **2011**, *32*, 8048–8057.
- (10) Kilian, K. A.; Mrksich, M. Directing Stem Cell Fate by Controlling the Affinity and Density of Ligand–Receptor Interactions at The Biomaterials Interface. *Angew. Chem., Int. Ed.* **2012**, *51*, 4891–4895.
- (11) Hubbell, J. A.; Schense, J. C.; Bloch, J.; Aebischer, P. Enzymatic Incorporation of Bioactive Peptides into Fibrin Matrices Enhances Neurite Extension. *Nat. Biotechnol.* **2000**, *18*, 415–419.
- (12) Wischerhoff, E.; Uhlig, K.; Lankenau, A.; Borner, H. G.; Laschewsky, A.; Duschl, C.; Lutz, J. F. Controlled Cell Adhesion on PEG–Based Switchable Surfaces. *Angew. Chem., Int. Ed.* **2008**, *47*, 5666–5668.
- (13) Chan, E. W. L.; Park, S.; Yousaf, M. N. An Electroactive Catalytic Dynamic Substrate That Immobilizes and Releases Patterned Ligands, Proteins, and Cells. *Angew. Chem., Int. Ed.* **2008**, *47*, 6267–6271.
- (14) Chen, H. B.; Xiao, L.; Anraku, Y.; Mi, P.; Liu, X. Y.; Cabral, H.; Inoue, A.; Nomoto, T.; Kishimura, A.; Nishiyama, N.; Kataoka, K. Polyion Complex Vesicles for Photoinduced Intracellular Delivery of Amphiphilic Photosensitizer. *J. Am. Chem. Soc.* **2014**, *136*, 157–163.
- (15) Yuan, Z. F.; Zhao, D.; Yi, X. Q.; Zhuo, R. X.; Li, F. Steric Protected and Illumination–Activated Tumor Targeting Accessory for Endowing Drug–Delivery Systems with Tumor Selectivity. *Adv. Funct. Mater.* **2014**, *24*, 1799–1807.
- (16) Nakanishi, J.; Kikuchi, Y.; Takarada, T.; Nakayama, H.; Yamaguchi, K.; Maeda, M. Photoactivation of a Substrate for Cell Adhesion under Standard Fluorescence Microscopes. *J. Am. Chem. Soc.* **2004**, *126*, 16314–16315.
- (17) Gong, Y. H.; Li, C.; Yang, J.; Wang, H. Y.; Zhuo, R. X.; Zhang, X. Z. Photoresponsive “Smart Template” *via* Host–Guest Interaction for Reversible Cell Adhesion. *Macromolecules* **2011**, *44*, 7499–7502.
- (18) Nowakowski, G. S.; Dooner, M. S.; Valinski, H. M.; Mihaliak, A. M.; Quesenberry, P. J.; Becker, P. S. A Specific Heptapeptide From a Phage Display Peptide Library Homes to Bone Marrow and Binds to Primitive Hematopoietic Stem Cells. *Stem Cells* **2004**, *22*, 1030–1038.
- (19) Cao, F. Y.; Yin, W. N.; Fan, J. X.; Zhuo, R. X.; Zhang, X. Z. A Novel Function of BMHP1 and cBMHP1 Peptides to Induce the Osteogenic Differentiation of Mesenchymal Stem Cells. *Biomater. Sci.* **2015**, *3*, 345–351.
- (20) Yin, W. N.; Cao, F. Y.; Han, K.; Zeng, X.; Zhuo, R. X.; Zhang, X. Z. The Synergistic Effect of a BMP-7 Derived Peptide and Cyclic RGD in Regulating Differentiation Behaviours of Mesenchymal Stem Cells. *J. Mater. Chem. B* **2014**, *2*, 8434–8440.
- (21) Li, W.; Wang, J. S.; Ren, J. S.; Qu, X. G. Near-Infrared Upconversion Controls Photocaged Cell Adhesion. *J. Am. Chem. Soc.* **2014**, *136*, 2248–2251.
- (22) Cox, J. D.; Curry, M. S.; Skirboll, S. K.; Gourley, P. L.; Sasaki, D. Y. Surface Passivation of a Microfluidic Device to Glial Cell Adhesion: A Comparison of Hydrophobic and Hydrophilic SAM Coatings. *Biomaterials* **2002**, *23*, 929–935.
- (23) Huang, Q. L.; Cheng, A.; Antensteiner, M.; Lin, C. J.; Vogler, E. A. Mammalian Cell–Adhesion Kinetics Measured by Suspension Depletion. *Biomaterials* **2013**, *34*, 434–441.
- (24) Lee, T. T.; García, J. R.; Paez, J. I.; Singh, A.; Phelps, E. A.; Weis, S.; Shafiq, Z.; Shekaran, A.; del Campo, A.; García, A. J. Light-Triggered *In Vivo* Activation of Adhesive Peptides Regulates Cell Adhesion, Inflammation and Vascularization of Biomaterials. *Nat. Mater.* **2014**, *14*, 352–360.
- (25) Ye, K.; Wang, X.; Cao, L. P.; Li, S. Y.; Li, Z. H.; Yu, L.; Ding, J. D. Matrix Stiffness and Nanoscale Spatial Organization of Cell-Adhesive Ligands Direct Stem Cell Fate. *Nano Lett.* **2015**, *15*, 4720–4729.
- (26) Higuchi, A.; Ling, Q. D.; Hsu, S. T.; Umezawa, A. Biomimetic Cell Culture Proteins as Extracellular Matrices for Stem Cell Differentiation. *Chem. Rev.* **2012**, *112*, 4507–4540.
- (27) Lee, J. S.; Kim, K.; Lee, K.; Park, J. P.; Yang, K.; Cho, S. W.; Lee, H. Surface Chemistry of Vitamin: Pyridoxal 5′-Phosphate (Vitamin B6) as a Multifunctional Compound for Surface Functionalization. *Adv. Funct. Mater.* **2015**, *25*, 4754–4760.
- (28) Sun, H.; Feng, K.; Hu, J.; Soker, S.; Atala, A.; Ma, P. X. Osteogenic Differentiation of Human Amniotic Fluid–Derived Stem Cells Induced by Bone Morphogenetic Protein-7 and Enhanced by Nanofibrous Scaffolds. *Biomaterials* **2010**, *31*, 1133–1139.